

# Two adaptation processes in auditory hair cells together can provide an active amplifier

Andrej Vilfan\* and Thomas Duke

Cavendish Laboratory, Madingley Road, Cambridge CB3 0HE, UK†

(Dated: 15. May 2003)

The hair cells of the vertebrate inner ear convert mechanical stimuli to electrical signals. Two adaptation mechanisms are known to modify the ionic current flowing through the transduction channels of the hair bundles: a rapid process involves  $\text{Ca}^{2+}$  ions binding to the channels; and a slower adaptation is associated with the movement of myosin motors. We present a mathematical model of the hair cell which demonstrates that the combination of these two mechanisms can produce ‘self-tuned critical oscillations’, i.e. maintain the hair bundle at the threshold of an oscillatory instability. The characteristic frequency depends on the geometry of the bundle and on the  $\text{Ca}^{2+}$  dynamics, but is independent of channel kinetics. Poised on the verge of vibrating, the hair bundle acts as an active amplifier. However, if the hair cell is sufficiently perturbed, other dynamical regimes can occur. These include slow relaxation oscillations which resemble the hair bundle motion observed in some experimental preparations.

## Introduction

Hair cells of the inner ear detect mechanical stimuli by deflections of the hair bundle, which open tension-gated transduction channels in the cell membrane to admit cations from the endolymph. The current is mostly composed of potassium ions, but also includes a small quantity of calcium ions (Lumpkin et al., 1997). Experiments in which hair bundles are held at a fixed deflection, using a microneedle, have revealed two adaptation processes that modify the transduction current, causing it to decline with time (Holt and Corey, 2000; Holt et al., 2002; Howard and Hudspeth, 1987, 1988; Wu et al., 1999). The first, which can occur on a sub-millisecond time scale, is dependent on the concentration of  $\text{Ca}^{2+}$  in the endolymph. It is believed to be a consequence of  $\text{Ca}^{2+}$  entering the hair bundle and binding to the transduction channels, making them more likely to close. The second, which takes up to hundreds of milliseconds, is also dependent on  $\text{Ca}^{2+}$  concentration, and is thought to be caused by the movement of adaptation motors attached to the transduction channels, which adjusts the tension that gates them.

A number of experiments have demonstrated that hair bundles can generate active oscillations, both in preparations of dissected tissue (Benser et al., 1993; Crawford and Fettiplace, 1985; Martin et al., 2000) and *in vivo* (Manley et al., 2001). It has been shown on theoretical grounds that the active oscillatory mechanism can provide an explanation for the high sensitivity and sharp frequency selectivity of auditory receptors (Camalet et al., 2000; Choe et al., 1998; Eguiluz et al., 2000; Ospeck et al., 2001) if the system is poised on the

verge of spontaneous oscillation. This critical point corresponds to a Hopf bifurcation of the active dynamical system. It has been suggested that a feedback mechanism operates to maintain the system at the critical point where it is most sensitive, leading to the concept of *self-tuned critical oscillations*. (Camalet et al., 2000).

The purpose of this article is to provide a coherent model for the active amplifier in hair cells, based on the combined action of the two known adaptation mechanisms. In our model the interaction of  $\text{Ca}^{2+}$  ions with the transduction channels generates an oscillatory instability of the hair bundle. Working on a slower time scale, the adaptation motors act to tune this dynamical system to the critical point, at which it just begins to oscillate. The two adaptation mechanisms together constitute a dynamical system displaying a *self-tuned Hopf bifurcation* (Camalet et al., 2000). Poised at the oscillatory instability, the hair bundle is especially responsive to faint sounds.

Our model differs from two published models of hair-bundle oscillations. Choe, Magnasco and Hudspeth (1998) have previously proposed that channel reclosure induced by  $\text{Ca}^{2+}$  ions can generate a Hopf instability. In their scheme the oscillation frequency is controlled by the kinetics of the transduction channel. In our model the frequency of spontaneous oscillations is governed, instead, by the architecture of the bundle and by the rate at which the calcium concentration equilibrates. This is more consistent with the finding that the rate at which the transduction channel switches is faster than the characteristic frequency, especially in low-frequency hair cells (Corey and Hudspeth, 1983). Camalet et al. (2000) have suggested that the Hopf instability is generated by motor proteins in the kinocilium, and that regulation to the critical point is accomplished by a feedback mechanism involving calcium. Their model is thus the converse of that presented here, but shares the underlying feature of self-tuned criticality. The current model ac-

\*Present address: J. Stefan Institute, Jamova 39, 1000 Ljubljana, Slovenia

†Electronic address: av242@cam.ac.uk

cords better with the observation that some hair bundles lack a kinocilium and others do not change their behavior significantly when the kinocilium is interfered with (Martin et al., 2003).

In addition to demonstrating that the two adaptation processes can combine to provide an active amplifier, we derive expressions that indicate how properties like the characteristic frequency of critical oscillations, and the sensitivity of response to sound waves, depend on parameters like the bundle height and the number of stereocilia. We also investigate how the dynamics can be modified if conditions are perturbed, and show that the bundle can exhibit slow relaxation oscillations which differ in many aspects from critical oscillations, but resemble the active movements recently observed in experiments on hair cells from the frog sacculus (Martin and Hudspeth, 1999).

## Model

### Hair bundle

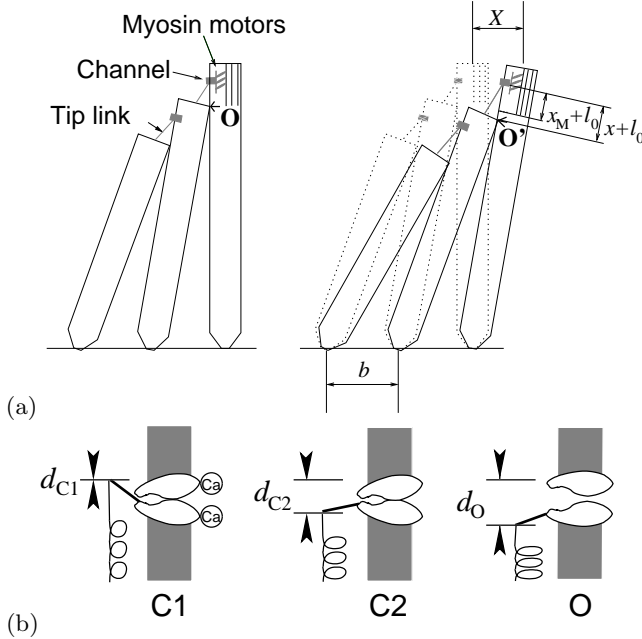


FIG. 1 (a) Schematic representation of a hair bundle. (b) Three-state model of the transduction channel. Note that  $\text{Ca}^{2+}$  binds to the channel when it is already in a closed state. The presence of  $\text{Ca}^{2+}$  therefore does not directly cause channel re-closure, but it does stabilize the closed state and delay re-opening.

Hair bundles in different species, or from hair cells with different characteristic frequencies within the same organ of the internal ear of a particular animal, can vary in shape and size, and also in the way that they are coupled to external mechanical vibrations (Hudspeth, 1997). Generally, one can distinguish between free-standing hair

bundles (e.g. some reptiles, mammalian inner hair cells) and those who tips are embedded in an accessory structure (e.g. other reptiles, birds, amphibial saccular hair cells). In experiments on dissected tissue, the accessory structure is usually removed. In this paper we will restrict our discussion to the simplest situation of a free-standing hair bundle. A bundle that is directly connected to the tectorial membrane could be described in a similar fashion, but using modified expressions for the stiffness, the friction and the coupling to the external signal.

The hair bundle (see Fig. 1a) is composed of  $N$  stereocilia which slope up against each other, the longest of which has length  $L$ . Typically,  $N$  and  $L$  are inversely related, with the range  $N = 20 - 300$  (Holt and Corey, 2000) corresponding to  $L = 30 - 2 \mu\text{m}$ . Each stereocilium is joined to the next by an elastic filament – the tip link – which connects to a tension-gated transduction channel in the cell membrane (Corey and Hudspeth, 1983; for a review see Markin and Hudspeth, 1995). The tension in the tip link can be adjusted by a group of myosin motors, which are connected to the transduction channel and move it along the actin filaments inside the stereocilium (Hudspeth and Gillespie, 1994).

To set up a coordinate system, we consider first a free-standing bundle. Within a stereocilium, we label the location at which the stereocilium touches its shorter neighbor  $\mathbf{O}$ . The position of the channel (and the attached motors) relative to  $\mathbf{O}$  is denoted by  $l_0 + x_M$ , where  $l_0$  is the length of a tip link at rest and  $x_M$  its extension under tension. When the tip of the bundle is deflected through a lateral displacement  $X$ , each stereocilium pivots at its base and adjacent stereocilia are sheared by a displacement  $\gamma X$ . The geometric factor  $\gamma$  may be written as  $\gamma \approx b/L$ , where  $b \approx 1 \mu\text{m}$  is the distance between the roots of neighboring stereocilia (Howard and Hudspeth, 1988; Howard et al., 1988). We label the new location at which the stereocilium touches its shorter neighbor  $\mathbf{O}'$ . The position of the channel relative to  $\mathbf{O}'$  is denoted by  $l_0 + x$ . It follows that

$$\gamma X = x - x_M. \quad (1)$$

The movement of the bundle is countered by an elastic restoring force, which has two contributions. First, the deformation of the stereocilia at their base provides an effective bundle stiffness  $K_{\text{SP}} = \kappa N/L^2$ , where  $\kappa$  is the pivotal stiffness of a stereocilium. The measured value  $\kappa \approx 1.5 \times 10^{-16} \text{ Nm/rad}$  (Crawford and Fettiplace, 1985; Hudspeth et al., 2000) indicates that  $K_{\text{SP}}$  varies from 0.01 pN/nm for tall bundles to 10 pN/nm for short ones. The second contribution, which scales in the same way with bundle size and is of similar magnitude, comes from the tension  $T_{\text{TL}}$  in the tip links. Movement of the bundle is also resisted by the viscous drag of the surrounding fluid which leads to a friction coefficient  $\zeta \sim \eta L$  for tall bundles, where  $\eta$  is the viscosity of the endolymph. Thus, when an external force  $F$  is applied to the tip of the bundle, its equation of motion is

$$\zeta \dot{X} = -N\gamma T_{\text{TL}}(x, C) - K_{\text{SP}}X + F, \quad (2)$$

(throughout the paper we use the convention  $\dot{X}(t) \equiv \frac{dX}{dt}$ ). Here, we have written  $T_{\text{TL}} = T_{\text{TL}}(x, C)$ , anticipating that the tension in the tip links depends on the local intracellular  $\text{Ca}^{2+}$  concentration  $C$ , as well as varying with the position  $x$ . For future reference, we note that the mechanical relaxation time of the hair bundle,  $\tau_{\text{mech}} = \zeta/K_{\text{SP}}$ , varies from a few microseconds to tens of milliseconds.

### Transduction channel

The mechanically-gated transduction channel is the central component of the model, since we postulate that hair bundle oscillations are driven by the force that is generated as the channels change conformation stochastically, as first suggested by Howard and Hudspeth (1988). It is generally assumed that transmembrane channel proteins can exist in a number of discrete states, some of which are closed and some open. As indicated in Fig. 1b, we additionally suppose that the channel protein incorporates a lever arm which amplifies the small structural changes that occur when the channel switches state, and thereby appreciably modifies the tension in the adjoining tip link (Martin et al., 2000). If  $p_i$  is the probability that the channel is in state  $i$ , and  $d_i$  is the position of the lever arm in that state, then the average tension may be written  $T_{\text{TL}} = \sum_i K_{\text{TL}}(x - d_i)p_i$ . Here,  $K_{\text{TL}}$  is the elastic constant of the tip link (or possibly that of a more compliant element in series with it (Kachar et al., 2000)), whose value obtained from micromechanical measurements is  $K_{\text{TL}} \approx 0.5 \text{ pN/nm}$  (Martin et al., 2000). In the steady state the probabilities  $p_i = w_i / (\sum_j w_j)$  are given by the Boltzmann factors  $w_i = \exp[-(\frac{1}{2}K_{\text{TL}}(x - d_i)^2 - G_i^0)/k_B T]$ , where  $G_i^0$  is the free energy of state  $i$ . Measurements of the transduction current as a function of bundle displacements in the frog's sacculus are well fitted with a three-state model of the channel (Corey and Hudspeth, 1983), with two closed states ( $i = \text{C1}, \text{C2}$ ) and one open state ( $i = \text{O}$ ). The fit indicates that the lever-arm movement is about 5 times greater for the transition  $\text{C1} \rightarrow \text{C2}$  than for the transition  $\text{C2} \rightarrow \text{O}$ , while more recent data (Martin et al., 2000) suggests that the total movement is about 8 nm. We therefore assign the lever arm displacements  $d_{\text{C1}} = 0 \text{ nm}$ ,  $d_{\text{C2}} = 7 \text{ nm}$  and  $d_{\text{O}} = 8.5 \text{ nm}$ . The free energies  $G_i^0$  depend on the local  $\text{Ca}^{2+}$  concentration  $C$  within the stereocilia (Howard and Hudspeth, 1988), which is strongly influenced by the entry of  $\text{Ca}^{2+}$  ions through the channel (Lumpkin and Hudspeth, 1995). A higher  $\text{Ca}^{2+}$  concentration favors closure of the channel, thereby providing a negative feedback. We model this dependence empirically, according to experimental observations (Corey and Hudspeth, 1983), as an effective shift in the channel gating point proportional to the logarithm

of the  $\text{Ca}^{2+}$  concentration

$$p_i(x, C) = p_i(x - x_s(C)) , \quad x_s(C) = D \ln \frac{C}{C_0} , \quad (3)$$

where the constant  $D$  has an empirical value of about 4 nm in the bullfrog's sacculus (Corey and Hudspeth, 1983) and  $C_0$  is the  $\text{Ca}^{2+}$  concentration in the free-standing bundle. One possible interpretation of this functional form, indicated in Fig. 1b, is that  $\text{Ca}^{2+}$  binds to state C2, causing it to switch to state C1 and thereby stabilizing the closed state. We emphasize that our model does not rely on the channel having three states. A two-state channel (eliminating state C2) would give substantially similar results.

An important aspect of our model is that we assume that the channel kinetics are rapid compared to the bundle oscillations and the calcium dynamics. The evidence for this assumption comes, for instance, from saccular hair cells that detect frequencies up to 150 Hz and have channel opening times around 100  $\mu\text{s}$  (Corey and Hudspeth, 1983). We can therefore consider the different channel states to be thermally equilibrated with one another, and chemically equilibrated with the  $\text{Ca}^{2+}$  ions. Then we can split the tip link tension  $T_{\text{TL}}$  into two components:  $K_{\text{TL}}x$ , the passive elastic force that the tip link would contribute in the absence of the transduction channel; and  $f$ , the active contribution arising from the channel switching states, also called *gating force*:

$$T_{\text{TL}}(x, C) = K_{\text{TL}}x + f(x - x_s(C)) , \quad (4)$$

where  $f(x, C) = -\sum_i K_{\text{TL}}d_i p_i(x, C)$ . A relationship between the gating force and the channel opening probability, which holds in any model with a single open state, reads  $f(x, C) \equiv k_B T \frac{\partial(\ln p_{\text{O}}(x, C))}{\partial x} - K_{\text{TL}}d_{\text{O}}$  (van Netten and Kros, 2000).

### Calcium dynamics

The dynamics of the calcium concentration in a stereocilium is influenced by a number of processes. As well as the influx of  $\text{Ca}^{2+}$  through the transduction channel, there is an outflux due to calcium pumps. The ions also diffuse freely, or in association with mobile buffers, and can additionally bind to fixed buffers. A detailed model of this dynamics was developed by Lumpkin and Hudspeth (1998), but for our purposes it suffices to use a simplified linearized model in which the  $\text{Ca}^{2+}$  concentration on the inner side of the channel obeys the equation

$$\dot{C} = -\lambda [C - C_B - C_{\text{MPO}}(x, C)] . \quad (5)$$

Here  $C_B$  is the steady-state concentration which would occur if the channel were blocked, originating from diffusion from other parts of the cell;  $C_M$  is the maximal additional contribution from influx through an open

transduction channel, and is of order  $10\mu\text{M}$ . The relaxation rate of calcium concentration fluctuations,  $\lambda$ , is an important parameter in our model. We expect the relaxation time  $\tau_{\text{chem}} = 1/\lambda$  to be of the order of milliseconds, corresponding to the measured fast adaptation time (Ricci and Fettiplace, 1997). Note that the slow  $\text{Ca}^{2+}$  kinetics (along with fast channel switching) is a key difference between our model and that of Choe et al. (1998), where the converse situation is assumed. The slow  $\text{Ca}^{2+}$  dynamics might seem at odds with the fact that the binding sites on the channel are reached by the incoming ions very quickly. But in our model, the channel is in state C2 when  $\text{Ca}^{2+}$  binds, i.e. it is closed (Fig. 1b). It therefore typically senses a concentration which is determined by diffusion within a larger volume, and which also depends on the interaction of  $\text{Ca}^{2+}$  with fixed and mobile buffers. Because a  $\text{Ca}^{2+}$  ion binds to one of the buffers in less than  $1\mu\text{s}$  (Lumpkin and Hudspeth, 1998), the concentration of free  $\text{Ca}^{2+}$  equilibrates with that bound to the buffers within a few microseconds of channel closure  $\text{O} \rightarrow \text{C2}$ . The time-scale of  $\text{Ca}^{2+}$  relaxation is therefore determined by buffering, diffusion to distant parts of the stereocilium and the activity of  $\text{Ca}^{2+}$  pumps. Indeed, the influence of buffers on the fast adaptation process has been observed experimentally (Ricci and Fettiplace, 1997).

### Adaptation motors

Experiments in which a vertebrate hair bundle is suddenly displaced (Howard and Hudspeth, 1987; Wu et al., 1999) show a slow adaptation of the channel current, on the scale of tens of milliseconds. The transduction channel is attached to the actin cortex within a stereocilium by a number of myosin 1C (formerly I $\beta$ ) motors. There is strong evidence that these molecular motors mediate slow adaptation (Assad and Corey, 1992; Gillespie and Corey, 1997; Holt et al., 2002), presumably by maintaining the proper tension in the tip link (Hudspeth and Gillespie, 1994). For simplicity, we assume that the motors have a linear force-velocity relation, so that

$$\dot{x}_M = v_M \left[ 1 - \frac{T_{\text{TL}}}{n_M F_M} \right], \quad (6)$$

where  $n_M$  is the number of motors bound to the actin,  $F_M$  is the stall force of an individual motor and  $v_M$  is its zero-load velocity. We take values typical for a motor protein,  $F_M \approx 1\text{ pN}$  and  $v_M \approx 0.3\mu\text{m/s}$  and suppose that there are  $N_M \approx 20$  motors per channel (experimental data suggest  $N_M \lesssim 130$  (Gillespie and Hudspeth, 1993)).

Calcium has been shown to influence the action of the adaptation motor (Hacohen et al., 1989; Ricci et al., 1998), possibly by increasing its rate of detachment from actin. The number of bound motors is therefore not constant, but obeys the dynamical equation

$$\dot{n}_M = \omega_M [-n_M g(C) + (N_M - n_M)] . \quad (7)$$

where  $\omega_M \approx 200\text{ s}^{-1}$  is the myosin binding rate and  $g(C)$  is a function describing the dependence of the detachment rate on the  $\text{Ca}^{2+}$  concentration.

## Results and Discussion

### Linear stability analysis

In order to examine the dynamical stability of the hair bundle in the absence of a driving force,  $F = 0$ , we make use of the fact that the adaptation motors operate on a slower time scale than both the mechanical relaxation of the bundle and the relaxation of the calcium concentration. We can therefore neglect their motion for now, and suppose that  $x_M$  is fixed. This leaves two coupled first-order differential equations of motion: Eq. 5 (supplemented with Eq. 3) for the rate of change of  $\text{Ca}^{2+}$  concentration; and by combining Eqs. 1, 2 & 4, the following equation for the motion of the transduction channels:

$$\dot{x} = -\frac{1}{\zeta} \{ N\gamma^2 [K_{\text{TL}}x + f(x - x_s(C))] + K_{\text{SP}}(x - x_M) \} . \quad (8)$$

The system has one or more fixed points, given by  $\dot{x} = 0$  and  $\dot{C} = 0$ , whose stability can be determined from the Jacobian matrix

$$\mathbf{J} = \begin{pmatrix} \frac{\partial \dot{x}}{\partial x} & \frac{\partial \dot{C}}{\partial x} \\ \frac{\partial \dot{x}}{\partial C} & \frac{\partial \dot{C}}{\partial C} \end{pmatrix}, \quad (9)$$

which has trace and determinant

$$\text{Tr } \mathbf{J} = -\frac{1}{\zeta} [K_{\text{B}} + N\gamma^2 f'] - \lambda(1 + \mu), \quad (10)$$

$$\det \mathbf{J} = \frac{\lambda}{\zeta} [K_{\text{B}}(1 + \mu) + N\gamma^2 f'] , \quad (11)$$

(throughout the paper we use the convention  $f'(x) \equiv \frac{\partial f}{\partial x}$ ,  $p'_O(x) \equiv \frac{\partial p_O}{\partial x}$  and  $x'_s \equiv \frac{\partial x_s}{\partial C}$ ). Here,  $K_{\text{B}} = K_{\text{SP}} + N\gamma^2 K_{\text{TL}}$  is the combined passive elasticity of the bundle due to the stereocilia and the tip links; and  $\mu = C_M x'_s p'_O$  is a dimensionless combination of variables which has a value close to unity for the choice of channel parameters specified above (for  $C_{\text{B}} = 0$  it can also be expressed as  $\mu = D(f + K_{\text{TL}} d_O)/k_{\text{BT}}$ ). A fixed point is stable if both eigenvalues of  $\mathbf{J}$ , evaluated at the fixed point, have a negative real part. This is equivalent (Strogatz, 1994) to the two conditions:  $\det \mathbf{J} > 0$ , and  $\text{Tr } \mathbf{J} < 0$ . The number of fixed points is most readily appreciated by considering the form of Eq. 8 for the velocity  $\dot{x}$  as a function of displacement  $x$  (see Fig. 2). Two distinct situations can arise depending on the strength of the calcium feedback:

(i) Consider first the case of weak feedback, so that the  $\text{Ca}^{2+}$  concentration  $C$  in the stereocilia is approximately constant. Typically  $\dot{x}(x, C = \text{const})$  varies *non-monotonically* with  $x$ . This is a consequence of a region of effective *negative elasticity*, caused by the redistribution of the transduction channel states when the bundle is moved (Howard and Hudspeth, 1987; Martin et al.,

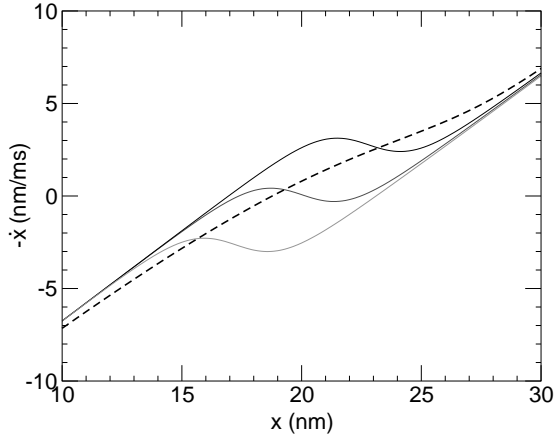


FIG. 2 Velocity  $\dot{x}$  as a function of displacement  $x$  for a fixed location of the motors  $x_M$ . If the  $\text{Ca}^{2+}$  concentration is held constant,  $\dot{x}(x, C = \text{const})$  typically has a region of negative slope (solid lines, for three different hypothetical values of  $C$ ). For a certain range of values of  $C$ , the system can then have three fixed points. But if the  $\text{Ca}^{2+}$  concentration is allowed to adjust, the curve  $\dot{x}(x, C = C(x))$ , where  $C(x)$  is the steady-state solution of Eq. 5, rises monotonically with  $x$  (dotted line). There is then a single fixed point. The channel parameters are  $G_{C1}^0 = 0$ ,  $G_{C2}^0 = 60 \text{ zJ}$ ,  $G_O^0 = 70 \text{ zJ}$ ,  $d_{C1} = 0 \text{ nm}$ ,  $d_{C2} = 7 \text{ nm}$ ,  $d_O = 8.5 \text{ nm}$  and  $D = 4 \text{ nm}$ . With these channel parameters  $K_{\text{TL}} d_O^2 \approx 9 k_B T$  (in a simplified two-state channel model neglecting the stereociliary stiffness  $K_{\text{SP}}$  the condition for the occurrence of a negative slope is  $K_{\text{TL}} d_O^2 > 4 k_B T$ ).

2000). At large displacements – both positive and negative – the tension  $T_{\text{TL}}$  in the tip links is determined by their passive elasticity. But at intermediate displacements, the occupancy of the closed state C1 declines rapidly with increasing  $x$ ; the resulting force  $f$ , caused by the swing of the lever arm, is negative and *reduces* the tension in the tip links so that  $T_{\text{TL}}$  decreases with increasing  $x$ . This effect has been termed ‘gating compliance’ by Howard and Hudspeth (1987). As indicated in Fig. 2, there will then be either one or three fixed points. According to the index theorem (Strogatz, 1994, Sect. 6.8) out of  $2n + 1$  fixed points,  $n$  will be saddle-points. Therefore, if the system has three fixed points, the central fixed point is a saddle point and the other two may be either stable or unstable. The number of fixed points depends on the values of the channel parameters, but also on the motor position  $x_M$ . Their stability depends additionally on the values of the dynamical model parameters ( $\zeta$  and  $\lambda$ ). A typical example of the location and nature of the fixed points, as a function of the motor position  $x_M$ , is shown in Fig. 3a; in this particular case, the bundle displays a region of *bistability*. We shall return to this situation later, to discuss the dynamical behavior of the hair bundle in recent *in vitro* experiments.

(ii) When the calcium feedback is operational, to determine the fixed points it is appropriate to consider the

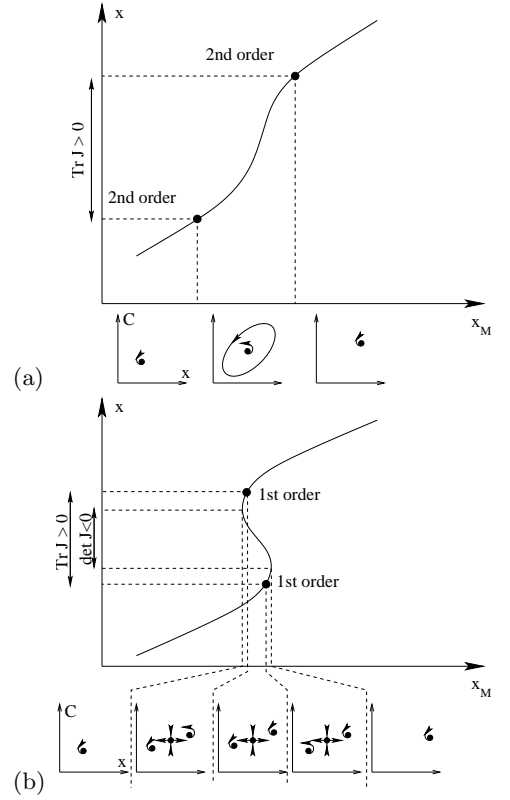


FIG. 3 Fixed points of the displacement  $x$  as a function of the location of the adaptation motors  $x_M$ . Trajectories in the plane  $(x, C)$  are indicated schematically below. (a) The situation with a weak  $\text{Ca}^{2+}$  feedback. The system displays a variety of dynamical regimes, including a region of bistability. (b) With strong  $\text{Ca}^{2+}$  feedback there is a single fixed point which becomes unstable (and encircled by a stable limit cycle) for an intermediate range of values of  $x_M$ . We expect the hair cells to use this regime *in vivo*.

curve  $\dot{x}(x, C = C(x))$ , where  $C(x)$  is the steady-state  $\text{Ca}^{2+}$  concentration at fixed  $x$ , given by  $\dot{C} = 0$  in Eq. 5. If the feedback is sufficiently strong,  $\dot{x}$  varies *monotonically* with  $x$  (Fig. 2); the readjustment of the channel states caused by the binding of  $\text{Ca}^{2+}$  ions provides a positive contribution to the active force  $f$ , eliminating the region of negative elasticity. The condition for this to occur is that  $\det \mathbf{J} > 0$  along the curve  $C(x)$ , or

$$\mu > -\frac{N\gamma^2}{K_B} f' - 1. \quad (12)$$

In this case, there is a single fixed point (Fig. 3b), which may be either stable (if  $\text{Tr } \mathbf{J} < 0$ ) or unstable (if  $\text{Tr } \mathbf{J} > 0$ ). In the latter situation, the bundle undergoes limit-cycle oscillations. Significantly, the stability depends on the location of the motors  $x_M$ , in addition to the values of the other model parameters. Typically the critical point at which  $\text{Tr } \mathbf{J} = 0$  is a *supercritical* Hopf bifurcation, which means that the system is continuously controllable, passing smoothly from the quiescent to the vibrating state as indicated in Fig. 4. Thus by moving

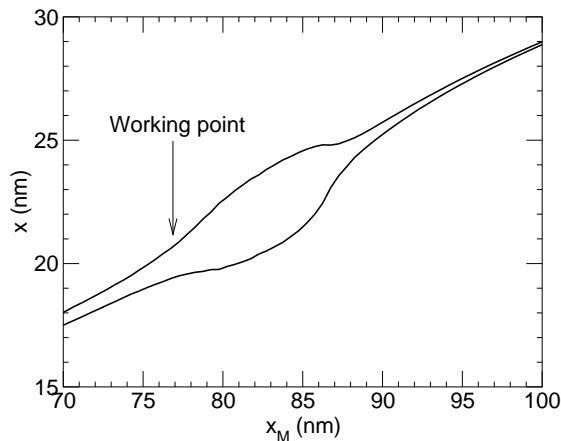


FIG. 4 Displacement  $x$  as a function of the location of the adaptation motors  $x_M$ , for the proposed *in vivo* situation corresponding to Fig. 3b. Between the two bifurcation points,  $x$  oscillates between a minimum and a maximum value shown by the two curves. The motor-mediated self-tuning mechanism (see text) maintains the system at a working point close to the first Hopf bifurcation. This result was obtained from a stochastic simulation with full channel kinetics, but in the absence of external (thermal) noise. The upper and lower line show the average maximum and minimum values of the displacement during one period of oscillation. Note that even in the quiescent phase the amplitude is non-zero, due to channel noise. The noisy motion in the quiescent phase has a very different spectrum from the oscillating phase, however.

along the stereocilia, the motors can determine whether the bundle stays still, or with what amplitude it oscillates spontaneously.

### Frequency of limit-cycle oscillations

We propose that the regime of strong calcium feedback, in which the bundle can oscillate spontaneously, is the regime that is relevant for auditory hair cells in normal physiological conditions. The control parameter that determines the stability of the bundle is  $\epsilon = \frac{1}{2} \text{Tr } \mathbf{J}$  and the Hopf bifurcation occurs at  $\epsilon = 0$ . It is worth emphasizing that within the scope of a non-inertial model with two variables ( $x$  and  $C$ ), in order for the bundle to oscillate spontaneously, it is essential that either the bundle displays a region of negative elasticity at constant  $\text{Ca}^{2+}$  concentration, or that there is a positive feedback in the  $\text{Ca}^{2+}$  dynamics. The second option would imply that an increase in the intracellular  $\text{Ca}^{2+}$  concentration would enhance the  $\text{Ca}^{2+}$  inflow, which contradicts the present experimental evidence. Our model only allows for the first option and from Eq. 10 it can be seen that the critical condition  $\epsilon = 0$  requires that  $K_B + N\gamma^2 f' < 0$ , i.e. the passive bundle stiffness must be more than compensated by the gating compliance. Negative elasticity has been measured in hair cells of the bullfrog sacculus (Martin et al., 2000), and has been interpreted as being

due to gating compliance (Howard and Hudspeth, 1987) as discussed above.

For small, positive values of  $\epsilon$ , the bundle executes small-amplitude limit-cycle oscillations of frequency  $\omega_C = \sqrt{\det \mathbf{J}}$ . From Eq. 11 it follows that the characteristic frequency of the hair bundle scales as

$$\omega_C \sim \sqrt{\lambda \frac{K_B}{\zeta}} \propto \sqrt{\lambda \frac{N}{L^3}} \quad (13)$$

Note that the period of oscillation  $T_C$  is approximately given by the geometric mean of the two relaxation times,  $T_C \sim \sqrt{\tau_{\text{mech}} \tau_{\text{chem}}}$ . Little is known about the variability of the calcium relaxation rate  $\lambda$ . If it is constant from cell to cell, the characteristic frequency is determined only by the bundle geometry. For the range of bundle sizes found e.g. in the chick's cochlea ( $L = 1.5 - 5.5 \mu\text{m}$ ,  $N = 300 - 50$  (Tilney and Saunders, 1983)), the frequency of the shortest bundles would then be approximately 17 times greater than the frequency of the tallest bundles. This is somewhat lower than the measured frequency range (about 50 Hz to 5 kHz (Manley et al., 1991)). We note, however, that to ensure the existence of an oscillatory instability for all hair cells,  $\epsilon = 0$  from Eq. 10 must be fulfilled for each cell. In addition, a strong mismatch between  $\tau_{\text{mech}}$  and  $\tau_{\text{chem}}$  would seriously limit the range of amplitudes for which active amplification can be maintained. This suggests that  $\lambda$  may vary with the geometry of the cell; ideally it would scale as  $\lambda \sim K_B/\zeta$ , i.e.  $\tau_{\text{chem}} \sim \tau_{\text{mech}}$ . Such variation could be achieved by a differential level of expression of calcium pumps or different buffer concentrations. In this case, the range would be enhanced to cover frequencies differing by a factor of 200. In what follows, we shall assume that this scaling (which is equivalent to  $\lambda \sim \omega_C$ ) holds. Note that in contrast to the model proposed by Choe, Magnasco and Hudspeth (1998) no variation of transduction channel kinetics is necessary in order to achieve a broad range of characteristic frequencies. Instead a simultaneous variation of the hair bundle geometry and the  $\text{Ca}^{2+}$  relaxation rate is required.

### Critical oscillations

It has been proposed on general theoretical grounds that the frequency selectivity of hair bundles, as well as their sensitivity to weak signals, is conferred by their proximity to a dynamical instability (Camalet et al., 2000; Eguiluz et al., 2000). Poised on the verge of oscillating at a characteristic frequency  $\omega_C$ , a hair bundle is especially responsive to periodic disturbances at that frequency. To ensure robust operation, a control system is required which maintains the hair bundle close to the critical point at which it just begins to vibrate. The general concept of a self-tuned Hopf bifurcation was therefore introduced (Camalet et al., 2000), whereby an appropriate feedback mechanism automatically tunes the system to the vicinity of the critical point. For the mo-

ment, we will assume that this mechanism works effectively, so that each hair cell is poised at a working point very close to its critical point, as indicated in Fig. 4.

In the vicinity of the bifurcation the limit cycle can be described by expanding the equations of motion about the fixed point as a power series, keeping terms up to third order. It is convenient to introduce a complex variable

$$\mathcal{Z} = \Delta x + \alpha \Delta C, \quad (14)$$

where  $\Delta x$  and  $\Delta C$  measure the difference of  $x$  and  $C$  from their respective values at the critical point. With the choice

$$\alpha = \frac{J_{22} - \epsilon + i\omega_C}{J_{12}}, \quad (15)$$

where  $J_{12} = \lambda C_M p'_O$  and  $J_{22} = -\lambda(1 + \mu)$  (Eq. 9), the equations of motion can be written as

$$\dot{\mathcal{Z}} = (\epsilon + i\omega_C)\mathcal{Z} + \mathcal{Q} + \mathcal{B}|\mathcal{Z}|^2\mathcal{Z} + \mathcal{C}, \quad (16)$$

where  $\mathcal{Q}$  represents all quadratic terms and  $\mathcal{C}$  all remaining cubic terms. The expression for the coefficient  $\mathcal{B}$  is given in the Appendix; for typical parameters,  $\text{Re}\mathcal{B}$  is negative, in which case the bifurcation is supercritical and therefore continuously controllable. To leading order, the amplitude of the variable  $\mathcal{Z}$  is then given by  $\mathcal{A} = \sqrt{-\epsilon/\text{Re}\mathcal{B}}$ , while all other terms cause only perturbations to the trajectory (Wiggins, 1990). The solution for spontaneous critical oscillations therefore reads

$$\Delta x(t) = \frac{\text{Im}(\alpha \bar{\mathcal{Z}}(t))}{\text{Im}\alpha}, \quad \Delta C(t) = \frac{\text{Im}\mathcal{Z}(t)}{\text{Im}\alpha}, \quad \mathcal{Z}(t) = \mathcal{A}e^{i\omega_C t} \quad (17)$$

and the oscillation amplitude of  $\Delta x$  is  $\frac{|\alpha|}{\text{Im}\alpha}\mathcal{A}$ .

### Critical response to sound waves

Sound waves or other vibrations entering the inner ear cause flow in the fluid surrounding the hair bundles. If the (unperturbed) fluid motion at the height of the bundle tip has amplitude  $A$  and frequency  $\omega$ , the force exerted on the bundle tip in Eq. 2 is  $F = A\omega\zeta_{\text{flow}}\cos(\omega t)$ . Here,  $\zeta_{\text{flow}} \sim \eta L$  is the friction coefficient of a stationary bundle in a flowing fluid. Note that  $\zeta_{\text{flow}}$  is not precisely equal to  $\zeta$ , which is the friction coefficient of the bundle moving in a stationary flow, because the latter also includes a contribution from shear flow between the stereocilia. This contribution scales as  $\sim \eta L \times N\gamma^2$  and is negligible for tall bundles but might become significant for short thick bundles. To preserve generality we write  $\zeta_{\text{flow}}/\zeta = \nu$ , where  $\nu$  is a constant of order unity which might vary with bundle geometry.

The external force leads to an additional driving term on the right hand side of Eq. 16, given by

$$\mathcal{F} = \frac{1}{2}A\omega\gamma\nu e^{i\omega t}. \quad (18)$$

For sound frequencies close to the characteristic frequency of the bundle,  $\omega \approx \omega_C$ , and amplitudes larger than the thermal noise, the response of the system is

$$\mathcal{Z} = \sqrt[3]{\frac{|\mathcal{F}|}{-\text{Re}\mathcal{B}}} e^{i\omega t}, \quad (19)$$

where we have assumed that the bundle is poised precisely at the Hopf bifurcation,  $\epsilon = 0$ .

Using the estimate  $\text{Re}\mathcal{B} \sim -\omega_C/d_O^2$  (see Appendix) we obtain

$$\Delta x \sim \sqrt[3]{\gamma\nu A d_O^2} = \sqrt[3]{\nu A d_O^2 b/L}. \quad (20)$$

This is the strongly compressive response characteristic of a Hopf resonance (Camalet et al., 2000; Eguiluz et al., 2000). Displacements of the transduction channel which produce a resolvable response,  $\Delta x = 1 - 10$  nm, typically correspond to wave amplitudes  $A = 1 - 1000$  nm in the fluid.

For weak stimuli, it is important to take the effects of noise into consideration. The buffeting of the hair-bundle by the Brownian motion in the surrounding fluid will render the spontaneous critical oscillations noisy. In this regime, signals that yield a response that is smaller than the spontaneous motion can nevertheless be detected, owing to phase-locking of the noisy oscillations (Camalet et al., 2000). The ability to detect phase locking in neural signals despite no increase in the firing rate has been experimentally confirmed in a number of species (Narins and Wagner, 1989). In the Appendix we provide an argument for the threshold of detection which suggests that for high frequency bundles containing many stereocilia, the smallest wave amplitude that can be detected may be as small as  $A \approx 0.1$  nm.

### Self-tuning mechanism

In order to achieve the combination of frequency selectivity, amplification of weak signals and wide dynamic range, the system has to be tuned to the close proximity of the Hopf bifurcation ( $\text{Tr}\mathbf{J} = 0$  in Eq. 10). We propose that this is accomplished by a feedback control mechanism which is mediated by the adaptation motors. The basic requirement is that when the hair bundle is still, the force exerted by the motors gradually increases so that they advance up the stereocilia (increasing  $x_M$ ), pushing the system into the unstable regime (see Fig. 4); but when the bundle is oscillating, the motor force gradually declines, so that the motors slip back down the stereocilia, returning the system to the quiescent state. It would appear that some type of high-pass or band-pass filter, which can detect whether or not the bundle is oscillating, must form an integral part of the feedback mechanism that controls the motors.

It has long been known that the hair cells of some vertebrates have, in their cell membranes, a system of potassium channels (BK) and voltage-gated calcium channels

that display a resonant response to oscillating input currents (Hudspeth and Lewis, 1988). It has been suggested that their purpose is to sharpen the tuning of the signal passed to the auditory nerve (Crawford and Fettiplace, 1980). It has alternatively been postulated that this system may itself generate self-sustained Hopf oscillations (Ospeck et al., 2001) and could be the basis of active bundle movement. We put forward a further possibility: One role of this system of channels is to detect bundle oscillations and to control the adaptation motors via a flux of calcium ions into the hair bundle (in fact, it is more likely that the motors are regulated by  $\text{Ca}^{2+}$ -controlled secondary messengers diffusing into the hair bundle, rather than by  $\text{Ca}^{2+}$  directly, but this would not qualitatively alter the following argument).

We model the filtering characteristic of the electrical oscillator by a Lorentzian transmission function

$$V(\omega) = V_0 + I_{\text{input}}(\omega) R_F \frac{\omega_F^2}{\omega_F^2 - \omega^2 + i\omega\omega_F/Q} \quad (21)$$

where  $V$  is the receptor potential,  $R_F$  is a channel resistance and  $I_{\text{input}} \propto p_O$  is the transduction current. The mechanism operates best if the filter frequency  $\omega_F$  equals the characteristic frequency  $\omega_C$  of hair-bundle oscillations, but this matching has to be encoded genetically or achieved by some mechanism beyond the scope of our model. With the value  $Q \approx 10$  measured experimentally in the bullfrog's sacculus (Hudspeth and Lewis, 1988), the filter distinguishes sufficiently well between the oscillating component of the transduction current and the underlying background level. The voltage-gated calcium channels then provide a  $\text{Ca}^{2+}$  flux varying (for example) exponentially with the membrane potential, which in turn determines the offset concentration in the stereocilia  $C_B$ , which appears in Eq. 5. We model it with the following differential equation

$$\dot{C}_B = I_{\text{Ca}} \frac{1}{1 + \exp(-q(V - V_{\text{Ca}})/k_B T)} - \lambda_B C_B, \quad (22)$$

where the parameters  $q$  and  $V_{\text{Ca}}$  describe the voltage sensitivity of the  $\text{K}_{\text{Ca}}$  channels,  $I_{\text{Ca}}$  is a measure of these channels' contribution to the  $\text{Ca}^{2+}$  flux in the region close to the transduction channel, and  $\lambda_B$  is the relaxation rate of the  $\text{Ca}^{2+}$  current. For the operation of tuning mechanism it is essential that  $\lambda_B \ll \omega_C$ . The contribution of  $C_B$  is insignificant when the bundle is quiescent, but grows rapidly if the bundle starts to oscillate.

The  $\text{Ca}^{2+}$  flowing into the bundle from the cell body regulates the oscillations in two ways. First, it reduces the control parameter of the bifurcation directly, Eq. 10. Second,  $\text{Ca}^{2+}$  ions binding to the myosin motors enhance their rate of detachment, via the function  $g(C)$  in Eq. 7, thereby regulating the total force that the team of motors produces. Here we take  $g(C) \propto C^3$ ; the precise functional form is not very important.

As shown in Fig. 5, this feedback control mechanism can successfully tune the system to the immediate vicinity of the Hopf bifurcation. In the absence of a sound

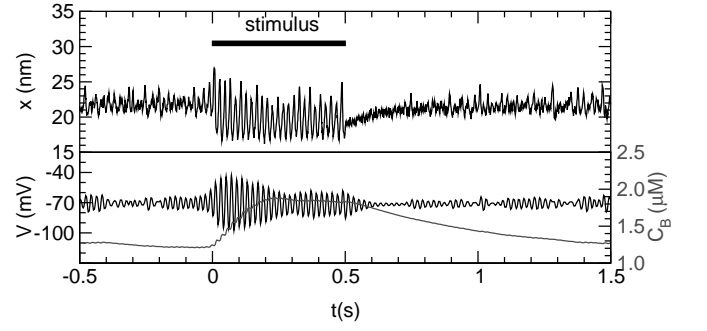


FIG. 5 Self-tuned critical oscillations. In the absence of a stimulus, the bundle performs noisy oscillations with a small amplitude. A strong external stimulus elicits a response that can detune the system for some time. Parameters values:  $N = 50$ ,  $K_{\text{TL}} = 0.5 \text{ pN/nm}$ ,  $K_{\text{SP}} = 0.15 \text{ pN/nm}$ ,  $\zeta = \zeta_{\text{flow}} = 0.65 \text{ pN ms/nm}$ ,  $\gamma = 0.14$  and  $A = 40 \text{ nm}$  ( the values of other parameters are listed in the last section of the Appendix ).

stimulus, a bundle executes noisy, self-tuned critical oscillations of low amplitude. If a strong stimulus is then applied, the bundle displays the characteristic response given by Eq. 20. The significant flow of  $\text{Ca}^{2+}$  into the cell elicited by this response detunes the system, so that when the stimulus is cut, the bundle falls still. Gradually, however, the motor-mediated self-tuning mechanism returns the system to its working point, where critical oscillations just set in, and where the hair bundle's sensitivity is maximal.

The hypothesis that the self-tuning mechanism is based on the detection of oscillations in the transduction current could be tested experimentally by disabling the electrical oscillations in the cell body. This could be done by voltage-clamping the cell or by specifically blocking, for example, the voltage-gated calcium channels. This would disable the self-tuning mechanism and therefore augment the bundle oscillations. On the other hand, if the electrical resonance is involved in the generation of oscillations, disabling it should eliminate the spontaneous bundle activity.

### Slow relaxation oscillations

The self-tuning mechanism described above is sufficiently robust to adjust the hair bundle to the critical point despite the natural variation of conditions that is likely to occur *in vivo*. Many experimental

preparations, however, involve significant perturbation from natural conditions, and this may shift the system into a different dynamical regime. In the following, we consider a particular type of dynamical behavior that can arise when the calcium feedback is weak. In this situation, as previously discussed in Fig. 3a, the interaction of the transduction channels with the calcium flux can produce a bistable system. If the position  $x_M$  of the adaptation motors is fixed, the hair bundle will settle at one or



other of the stable positions. However, this state of affairs is upset by the slow calcium feedback acting on the motors (Eq. 7). Suppose, for example, that the bundle is at the fixed point with the higher value of  $x$ , for which there is a high probability that the transduction channels are open. The  $\text{Ca}^{2+}$  ions entering through the channel bind to the motors, causing a fraction of them to detach, and the diminishing force exerted by the motors causes the tension in the tip links  $T_{\text{TL}}$  to fall. As indicated in Fig. 6a, the fixed point vanishes at a critical value of  $T_{\text{TL}}$ , and the system then abruptly jumps to the other fixed point. At this lower value of  $x$ , the channels are mostly closed. The resulting drop in calcium concentration augments the number of bound motors, increasing the tension in the tip links until the lower fixed point becomes unstable, whereupon the hair bundle jumps back to its initial position.

The consequence of this dynamics is a slow relaxation oscillation (Strogatz, 1994, Sect. 7.5) of the bundle deflection  $X$ , which has a non-sinusoidal form: each abrupt jump in position is followed by an interval of slow motion, as shown in Fig. 6b. Martin, Mehta and Hudspeth (2000) have observed oscillations of this type in their preparations of dissected tissue. They attributed the dynamical behavior to precisely the motor-mediated mechanism that we discuss here, and speculated that these oscillations form the basis of mechanical amplification of auditory stimuli. According to our model however, the relaxation oscillations differ in many respects from the Hopf oscillations which provide active amplification. They are considerably slower; their frequency is strongly amplitude-dependent; and the frequency does not significantly depend on the viscous relaxation time of the bundle, but is principally governed by the motors' sensitivity to changing calcium levels. In our model, relaxation oscillations are an accidental consequence of the self-tuning mechanism when the system is too far from normal operating conditions.

In the light of our analysis, various interpretations of the experiment of Martin, Mehta and Hudspeth 2000 are possible. It may be that in saccular hair cells, which are designed to detect low frequency vibrations, slow motor-mediated relaxation oscillators are sufficient to provide a rudimentary amplification of signals. Another possibility is that the observed oscillations can be adjusted to the vicinity of a Hopf bifurcation by some mechanism that we have not considered here, e.g. by alternating the bundle stiffness. A third possibility to bear in mind is that the conditions in preparations of dissected tissue are not precisely the same as those *in vivo*, and thus the hair bundles may not be operating in the dynamical regime that is physiologically relevant. Careful adjustment might permit the channel adaptation and the motor-mediated self-tuning mechanism to work together as we propose they do in auditory hair cells, in which case more rapid, critical Hopf oscillations might be observed.

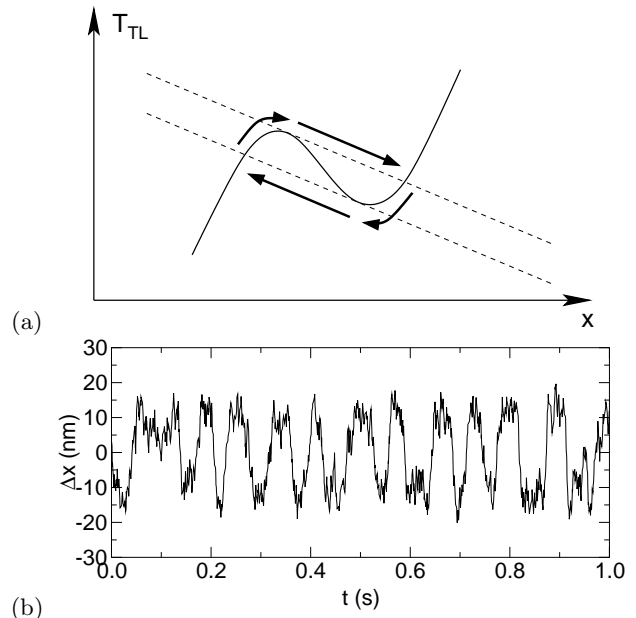


FIG. 6 Slow relaxation oscillator regime. (a) The solid line shows the tension-displacement relation for a channel, the dashed lines the contribution to tension from the passive bundle stiffness (which depends on the position of adaptation motors). In a quasistationary state these two must be equal. For a given position of the adaptation motors, there can be two stable solutions. The motors then move the system from one fixed point to the other. (b) Relaxation oscillations have a lower frequency than and a different shape from the critical oscillations. To achieve this regime the  $\text{Ca}^{2+}$  concentration outside the bundle was reduced and the self-tuning mechanism was replaced by a constant  $\text{Ca}^{2+}$  flow from the cell body.

## Conclusion

Our phenomenological model illustrates that the two adaptation processes which have been documented in hair cells can, together, generate a self-tuned Hopf bifurcation. The feedback mechanism that accomplishes the self-tuning requires, in addition, a system to detect bundle oscillations. We have shown that this can be accomplished by the resonant response of the BK and voltage-gated  $\text{Ca}^{2+}$  channels which has been established experimentally in lower vertebrates. The spontaneous frequency  $\omega_C$  of a hair cell is specified principally by the architecture of its hair bundle. To ensure robust operation of a hair cell, we expect that both the calcium relaxation rate  $\lambda$ , and the resonant frequency of the electrical oscillator are quite closely matched to the spontaneous oscillation frequency  $\omega_C$ . The self-tuning mechanism can reliably keep the hair bundle poised on the verge of oscillating *in vivo*. But the perturbations in conditions which can occur in some experimental preparations may lead to quite different dynamical regimes. Thus, while recent experiments on hair cells of the bullfrog sacculus show promising signs of active amplification

(Martin and Hudspeth, 1999, 2001; Martin et al., 2001, 2000), they may well not yet have revealed the full potential of auditory hair cells to detect faint sounds.

## Appendix

### Series expansion

In this section we derive an analytical expression for the third-order coefficient  $\mathcal{B}$  in the complex equation of motion (Eq. 16). The Taylor expansion of  $\tilde{\mathcal{Z}}$  up to third order, with the use of a new variable  $\xi = \Delta x - \Delta x_s(C)$  can be derived from the equations of motion (Eqs. 5 and 8) and the definition of  $\mathcal{Z}$  (Eq. 14):

$$\begin{aligned} \dot{\mathcal{Z}} = & [\text{Linear terms in } \Delta x, \Delta C] \\ & - \frac{N\gamma^2}{\zeta} \left[ f' \xi + \frac{1}{2} f'' \xi^2 + \frac{1}{6} f''' \xi^3 \right] \\ & + \alpha \lambda C_M \left[ p'_O \xi + \frac{1}{2} p''_O \xi^2 + \frac{1}{6} p'''_O \xi^3 \right]. \end{aligned} \quad (23)$$

Expanding  $\xi$  as a Taylor series in  $\Delta x$  and  $\Delta C$ , expressing the latter in terms of  $\mathcal{Z}$  using Eq. 17

$$\begin{aligned} \xi = & \frac{(\alpha + x'_s) \bar{\mathcal{Z}} - (\bar{\alpha} + x'_s) \mathcal{Z}}{\alpha - \bar{\alpha}} - \frac{1}{2} x''_s \frac{(\mathcal{Z} - \bar{\mathcal{Z}})^2}{(\alpha - \bar{\alpha})^2} \\ & - \frac{1}{6} x'''_s \frac{(\mathcal{Z} - \bar{\mathcal{Z}})^3}{(\alpha - \bar{\alpha})^3} + \mathcal{O}(\mathcal{Z}^3) \end{aligned} \quad (24)$$

and collecting the real part of the terms containing  $\mathcal{Z}^2 \bar{\mathcal{Z}}$  yields

$$\begin{aligned} \text{Re } \mathcal{B} = & - \frac{N\gamma^2}{16\zeta(\text{Im } \alpha)^2} \left( -x''_s f'' + |\alpha + x'_s|^2 f''' \right) \\ & - \frac{\lambda C_M}{16(\text{Im } \alpha)^2} \left( x'''_s p'_O - x''_s (2 \text{Re } \alpha + 3x'_s) p''_O \right. \\ & \left. + x'_s |\alpha + x'_s|^2 p'''_O \right). \end{aligned} \quad (25)$$

Inserting  $\alpha = x'_s(-\lambda(1+\mu) + i\omega_C)/(\lambda\mu)$  from Eq. 15 gives

$$\begin{aligned} \text{Re } \mathcal{B} = & - \frac{(\lambda\mu)^2}{16(\omega_C x'_s)^2} \left( \frac{N\gamma^2}{\zeta} \left( -x''_s f'' \right. \right. \\ & \left. \left. + (x'_s)^2 \left( 1 + \frac{\omega_C^2}{(\lambda\mu)^2} \right) f''' \right) + \lambda C_M \left( x'''_s p'_O \right. \right. \\ & \left. \left. - x''_s x'_s (1 - 2/\mu) p''_O + (x'_s)^3 \left( 1 + \frac{\omega_C^2}{(\lambda\mu)^2} \right) p'''_O \right) \right) \end{aligned} \quad (26)$$

and using the specific form of  $\Delta x_s$ , given by Eq. 3, we finally obtain

$$\begin{aligned} \text{Re } \mathcal{B} = & - \frac{(\lambda\mu)^2}{16\omega_C^2} \left( \frac{N\gamma^2}{\zeta} \left[ \frac{f''}{D} + \left( 1 + \frac{\omega_C^2}{(\lambda\mu)^2} \right) f''' \right] \right. \\ & \left. + \frac{\lambda C_M}{C} \left[ \frac{2p'_O}{D} - (1 - 2/\mu) p''_O + D \left( 1 + \frac{\omega_C^2}{(\lambda\mu)^2} \right) p'''_O \right] \right). \end{aligned} \quad (27)$$

If we assume a matching between the  $\text{Ca}^{2+}$  relaxation rate and the characteristic bundle frequency,  $\lambda \sim \frac{K_B}{\zeta} \sim \omega_C$ , the position  $x$  of the bifurcation becomes independent of the characteristic frequency and so do the terms  $p_O$ ,  $f$  and all their derivatives, evaluated at the bifurcation. The third-order coefficient then scales as

$$\text{Re } \mathcal{B} \sim - \frac{\omega_C}{d_O^2}. \quad (28)$$

The parameters we use in our simulation give the value  $\text{Re } \mathcal{B} = -6.7 \omega_C / d_O^2$ .

### Noise

In order to determine the level of the smallest stimulus that a hair bundle can detect, stochastic fluctuations of the bundle must be taken into account. There are several sources of noise in the system. The most important is the Brownian force that the surrounding fluid exerts on the bundle. The noise resulting from the stochastic opening and closing of channels is less significant, as can be seen by considering a simplified two-state channel model. We denote the lever arm shift between the two states by  $d$ , the average dwell times as  $\tau_0$  and  $\tau_1$  and the probability of finding the channel in state 1 by  $p_1$ . Then the expectation value of the number of channels in state 1 is  $\langle n_1 \rangle = N p_1$ , and the variance is  $\langle \Delta n_1^2 \rangle = N p_1 (1 - p_1)$ . The fluctuation in the total force from all channels is  $\langle \Delta F^2 \rangle = (K_{\text{TL}} d)^2 \langle \Delta n_1^2 \rangle$ . The noise has the spectral density of a dichotomous process

$$S(\omega) = \frac{\zeta}{\gamma^2} k_B T_N \frac{1}{\pi (1 + (\omega \tau_C)^2)}. \quad (29)$$

It has the characteristic of a Brownian noise with an effective temperature  $k_B T_N = \frac{\gamma^2}{\zeta} (K_{\text{TL}} d)^2 N p_1 (1 - p_1) \tau_C \approx k_B T \omega_C \tau_C$ , where  $\tau_C = (\tau_0^{-1} + \tau_1^{-1})^{-1}$ . The second approximation is based on the estimates  $k_B T \sim K_{\text{TL}} d_O^2$  (from the condition for the negative stiffness) and  $\omega_C \sim N \gamma^2 K_{\text{TL}} / \zeta$  (Eq. 13 with  $\lambda \sim \omega_C$ ). Since the channel switching time is shorter than the period of the oscillations,  $\omega_C \tau_C \ll 1$ , it follows that the channel noise is negligible compared to the thermal noise. The same can be shown for the influence of stochastic channel opening on the  $\text{Ca}^{2+}$  concentration inside the stereocilia.

Taking the Brownian force exerted by the fluid into account, the equation of motion for the complex variable

$\mathcal{Z}$  becomes

$$\dot{\mathcal{Z}} = (\epsilon + i\omega_C)\mathcal{Z} + \mathcal{B}|\mathcal{Z}|^2\mathcal{Z} + \mathcal{F} + \frac{\gamma^2}{\zeta}F_N(t) \quad (30)$$

where  $F_N(t)$  represents white noise with the autocorrelation function  $\langle F_N(t)F_N(t') \rangle = [2\zeta k_B T / \gamma^2] \delta(t - t')$ . Writing  $\mathcal{Z}' = \mathcal{Z}e^{-i\omega t}$  (and taking the stimulus frequency to be equal to the characteristic frequency), this equation can be transformed to

$$\frac{\zeta}{\gamma^2}\dot{\mathcal{Z}}' = -\frac{\partial}{\partial \mathcal{Z}'}U(\mathcal{Z}') + F_N(t)e^{-i\omega t}, \quad (31)$$

$$U(\mathcal{Z}') = \frac{\zeta}{\gamma^2} \left( -\frac{\epsilon}{2}|\mathcal{Z}'|^2 - \frac{\text{Re}\mathcal{B}}{4}|\mathcal{Z}'|^4 - |\mathcal{F}|\mathcal{Z}' \right). \quad (32)$$

It can be further simplified if we replace the “rotating” noise  $F_N(t)e^{-i\omega t}$  (which reflects the fact that the noise only acts on the spatial coordinate and not on the  $\text{Ca}^{2+}$  concentration) with an averaged, homogeneous noise term. The averaged noise then has the temperature  $\frac{1}{2}T$  and Eq. 32 becomes a Langevin equation for a particle of friction coefficient  $\zeta/\gamma^2$ , moving in a potential  $U(\mathcal{Z}')$ . The equilibrium solution is the Boltzmann distribution  $P(\mathcal{Z}') \propto \exp(-U(\mathcal{Z}')/(\frac{1}{2}k_B T))$ . For a bundle that is tuned to the critical point ( $\epsilon = 0$ ), the mean-square fluctuation amplitude in the absence of a stimulus ( $\mathcal{F} = 0$ ) is

$$\langle \mathcal{Z}^2 \rangle = \sqrt{\frac{2k_B T \gamma^2}{\pi \zeta (-\text{Re}\mathcal{B})}} \sim \frac{d_O^2}{\sqrt{N}} \quad (33)$$

(in the second step we used the estimates  $\text{Re}\mathcal{B} \sim -\omega/d_O^2$  (Eq. 28) and  $k_B T \sim K_{\text{TL}}d_O^2$ , the condition for negative stiffness). Using the numerical parameter values we obtain

$$\langle \mathcal{Z}^2 \rangle \approx 0.13 \frac{d_O^2}{\sqrt{N}}.$$

Weak stimuli which evoke a response that is smaller than the stochastic fluctuations of the bundle, nevertheless cause phase-locking of the spontaneous bundle oscillations (Camalet et al., 2000; Martin and Hudspeth, 2001). The brain might detect such signals through periodicity in the spike-train elicited by individual hair cells, or via the synchronicity of spikes from neighboring hair cells, whose characteristic frequencies differ only slightly. In either case, the quantity of interest is the Fourier component of bundle oscillations at the sound frequency. With a finite stimulus force  $\mathcal{F}$ , the Fourier component is

$$\langle \mathcal{Z}e^{-i\omega t} \rangle = \sqrt{\frac{2}{\pi}} \frac{|\mathcal{F}|}{\sqrt{-\text{Re}\mathcal{B}k_B T \gamma^2 / \zeta}} \sim A\nu\sqrt{N}\frac{b}{L}. \quad (34)$$

We assume that signals can be detected provided that the signal-to-noise ratio,  $\langle \mathcal{Z}e^{-i\omega t} \rangle / \sqrt{\langle \mathcal{Z}^2 \rangle}$ , exceeds a

certain threshold value  $\rho$ . The smallest detectable amplitude of fluid motion then scales as

$$A_{\min} \sim \frac{\rho d_O}{\nu} \frac{L}{b} N^{-\frac{3}{4}} \quad (35)$$

or with our numerical parameter values

$$A_{\min} \approx 1.0 \frac{\rho d_O}{\nu} \frac{L}{b} N^{-\frac{3}{4}}.$$

Taking  $\rho \approx 0.2$ ,  $L/b \approx 3$ ,  $\nu \approx 1$ , and  $N \approx 200$  gives  $A_{\min} \approx 0.1$  nm for high frequency bundles containing many stereocilia.

### Simulation of self-tuned critical oscillations

The model parameters and their values, used in the simulation, are listed in Table I. The channels were simulated as described in the main text, using a three-state model with parameters  $G_{C1}^0 = 0$ ,  $G_{C2}^0 = 60$  zJ,  $G_O^0 = 70$  zJ,  $d_{C1} = 0$  nm,  $d_{C2} = 7$  nm,  $d_O = 8.5$  nm and  $D = 4$  nm. The transition rate between the states C1 and C2 and between C2 and O was modeled as  $r_{i \rightarrow j} = \tau_{\text{ch}}^{-1} \exp((G_i - G_j)/2k_B T)$ , with the free energy in each state  $G_i = \frac{1}{2}K_{\text{TL}}(x - x_s(C) - d_i)^2 + G_i^0$ .

The resonant filter was simulated using the differential equation corresponding to the filter characteristics given by Eq. 21

$$\ddot{V} = -\omega_F^2(V - V_0) - \frac{\omega_F}{Q}\dot{V} + (n_O/N - p_O^0)I_{\text{Input}}R_F\omega_F^2 \quad (36)$$

where  $n_O$  is the number of open transduction channels and the parameters  $R_F = 35$  mV/nA,  $I_{\text{Input}} = 0.5$  nA,  $Q = 10$ ,  $V_0 = -70$  mV,  $p_O^0 = 0.15$  and  $\omega_F = 2\pi \times 50$  s<sup>-1</sup>.

The calcium contribution from the cell body was modeled according to Eq. (22) with  $I_{Ca} = 10$   $\mu$ M/s,  $\lambda_B = 1$  s<sup>-1</sup>,  $V_{Ca} = -65$  mV,  $q/k_B T = 0.2$  mV<sup>-1</sup>.

The adaptation motors were modeled with stochastic attachment at a fixed rate  $\omega_M = 200$  s<sup>-1</sup> and detachment at a  $\text{Ca}^{2+}$ -dependent rate  $g(C)\omega_M$ , with  $g(C) = (0.1 \mu\text{M}^{-3}) \times C^3$ .

All differential equations were solved using the Euler method. The time step was 1  $\mu$ s.

### Acknowledgment

We would like to thank R. Fettiplace, G. Manley, P. Martin, and S. van Netten for helpful discussions and comments on the manuscript. A.V. is a European Union Marie Curie Fellow. T.D. is a Royal Society University Research Fellow.

### References

- Assad, J. A., and D. P. Corey. 1992. An active motor model for adaptation by vertebrate hair cells. *J. Neurosci.* 12:3291-3309.

TABLE I Parameter values, used in the simulation

Tip-link stiffness	$K_{TL}$	0.5 pN/nm	(Martin et al., 2000)
Channel states	$d_{C2}$	7 nm	
	$d_O$	8.5 nm	(Martin et al., 2000)
Channel state energies	$G_{C2}^0$	60 zJ	
	$G_O^0$	70 zJ	
Ca <sup>2+</sup> dependent gating point shift	$D$	4 nm	(Corey and Hudspeth, 1983)
Switching time	$\tau_{ch}$	50 $\mu$ s	(Corey and Hudspeth, 1983)
Distance between stereociliary roots	$b$	1 $\mu$ m	(Howard et al., 1988)
Bundle height	$L$	7 $\mu$ m	(Howard et al., 1988)
Geometric factor	$\gamma$	0.14	(Howard et al., 1988)
Pivotal stiffness of a stereocilium	$\kappa$	$1.5 \times 10^{-16}$ Nm/rad	(Hudspeth et al., 2000)
Number of stereocilia	$N$	50	(Martin et al., 2000)
Viscous friction	$\zeta$	0.65 pN ms/nm	
Ca <sup>2+</sup> relaxation rate	$\lambda$	100 s <sup>-1</sup>	
Channel contribution to the Ca <sup>2+</sup> concentration	$C_M$	7 $\mu$ M	(Lumpkin and Hudspeth, 1998)
Number of adaptation motors per channel	$N_M$	20	
Motor association rate	$\omega_M$	200 s <sup>-1</sup>	
Motor speed	$v_M$	0.3 $\mu$ m/s	
Motor stall force	$F_M$	1 pN	
Maximum transduction current	$I_{input}/N$	500 pA	(van Netten and Kros, 2000)
Filter resistance	$R_F$	35 mV/nA	
Filter Q-factor	$Q$	10	(Hudspeth and Lewis, 1988)
Filter frequency	$\omega_F$	$2\pi \times 50$ s <sup>-1</sup>	
Membrane potential	$V_0$	-70 mV	
Ca <sup>2+</sup> channels gating point	$V_{Ca}$	-65 mV	
Ca <sup>2+</sup> channels gating charge	$q$	$q/k_B T = 0.2$ mV <sup>-1</sup>	
Time constant of the slow feedback	$\lambda_B$	1 s <sup>-1</sup>	
Ca <sup>2+</sup> gain due to slow feedback	$I_{Ca^{2+}}$	10 $\mu$ M/s	

- Benser, M. E., N. P. Issa, and A. J. Hudspeth. 1993. Hair-bundle stiffness dominates the elastic reactance to otolithic-membrane shear. *Hear. Res.* 68:243-252.
- Camalet, S., T. Duke, F. Jülicher, and J. Prost. 2000. Auditory sensitivity provided by self-tuned critical oscillations of hair cells. *Proc. Natl. Acad. Sci. USA* 97:3183-3188.
- Choe, Y., M. O. Magnasco, and A. J. Hudspeth. 1998. A model for amplification of hair-bundle motion by cyclical binding of Ca<sup>2+</sup> to mechanoelectrical-transduction channels. *Proc. Natl. Acad. Sci. USA* 95:15321-15326.
- Corey, D. P., and A. J. Hudspeth. 1983. Kinetics of the receptor current in bullfrog saccular hair cells. *J. Neurosci.* 3:962-976.
- Crawford, A. C., and R. Fettiplace. 1980. The frequency selectivity of auditory nerve fibres and hair cells in the cochlea of the turtle. *J. Physiol.* 306:79-125.
- Crawford, A. C., and R. Fettiplace. 1985. The mechanical properties of ciliary bundles of turtle cochlear hair cells. *J. Physiol.* 364:359-379.
- Eguiluz, V. M., M. Ospeck, Y. Choe, A. J. Hudspeth, and M. O. Magnasco. 2000. Essential nonlinearities in hearing. *Phys. Rev. Lett.* 84:5232-5235.
- Gillespie, P. G., and D. P. Corey. 1997. Myosin and adaptation by hair cells. *Neuron* 19:955-958.
- Gillespie, P. G., and A. J. Hudspeth. 1993. Adenine nucleoside diphosphates block adaptation of mechanoelectrical transduction in hair cells. *Proc. Natl. Acad. Sci. USA* 90:2710-2714.
- Hacohen, N., J. A. Assad, W. J. Smith, and D. P. Corey. 1989. Regulation of tension on hair-cell transduction channels: displacement and calcium dependence. *J. Neurosci.* 9:3988-3997.
- Holt, J. R., and D. P. Corey. 2000. Two mechanisms for transducer adaptation in vertebrate hair cells. *Proc. Natl. Acad. Sci. USA* 97:11730-11735.
- Holt, J. R., S. K. Gillespie, D. W. Provance, K. Shah, K. M. Shokat, D. P. Corey, J. A. Mercer, and P. G. Gillespie. 2002. A chemical-genetic strategy implicates myosin-1c in adaptation by hair cells. *Cell* 108:371-381.
- Howard, J., and A. J. Hudspeth. 1987. Mechanical relaxation of the hair bundle mediates adaptation in mechanoelectrical transduction by the bullfrog's saccular hair cell. *Proc. Natl. Acad. Sci. USA* 84:3064-3068.
- Howard, J., and A. J. Hudspeth. 1988. Compliance of the hair bundle associated with gating of mechanoelectrical transduction channels in the bullfrog's saccular hair cell. *Neuron*

- 1:189-199.
- Howard, J., W. M. Roberts, and A. J. Hudspeth. 1988. Mechano-electrical transduction by hair cells. *Annu. Rev. Biophys. Biophys. Chem.* 17:99-124.
- Hudspeth, A. 1997. Mechanical amplification of stimuli by hair cells. *Curr. Opin. Neurobiol.* 7:480-486.
- Hudspeth, A. J., Y. Choe, A. D. Mehta, and P. Martin. 2000. Putting ion channels to work: mechano-electrical transduction, adaptation, and amplification by hair cells. *Proc. Natl. Acad. Sci. USA* 97:11765-11772.
- Hudspeth, A. J., and P. G. Gillespie. 1994. Pulling springs to tune transduction: adaptation by hair cells. *Neuron* 12:1-9.
- Hudspeth, A. J., and R. S. Lewis. 1988. A model for electrical resonance and frequency tuning in saccular hair cells of the bull-frog, *Rana catesbeiana*. *J. Physiol.* 400:275-297.
- Kachar, B., M. Parakkal, M. Kurc, Y. Zhao, and P. G. Gillespie. 2000. High-resolution structure of hair-cell tip links. *Proc. Natl. Acad. Sci. USA* 97:13336-13341.
- Lumpkin, E. A., and A. J. Hudspeth. 1995. Detection of  $\text{Ca}^{2+}$  entry through mechanosensitive channels localizes the site of mechano-electrical transduction in hair cells. *Proc. Natl. Acad. Sci. USA* 92:10297-10301.
- Lumpkin, E. A., and A. J. Hudspeth. 1998. Regulation of free  $\text{Ca}^{2+}$  concentration in hair-cell stereocilia. *J. Neurosci.* 18:6300-6318.
- Lumpkin, E. A., R. E. Marquis, and A. J. Hudspeth. 1997. The selectivity of the hair cell's mechano-electrical transduction channel promotes  $\text{Ca}^{2+}$  flux at low  $\text{Ca}^{2+}$  concentrations. *Proc. Natl. Acad. Sci. USA* 94:10997-11002.
- Manley, G. A., A. Kaiser, J. Brix, and O. Gleich. 1991. Activity patterns of primary auditory-nerve fibres in chickens: development of fundamental properties. *Hear. Res.* 57:1-15.
- Manley, G. A., D. L. Kirk, C. Koppl, and G. K. Yates. 2001. In vivo evidence for a cochlear amplifier in the hair-cell bundle of lizards. *Proc. Natl. Acad. Sci. USA* 98:2826-2831.
- Markin, V. S., and A. J. Hudspeth. 1995. Gating-spring models of mechano-electrical transduction by hair cells of the internal ear. *Annu. Rev. Biophys. Biomol. Struct.* 24:59-83.
- Martin, P., D. Bozovic, Y. Choe, and A. J. Hudspeth. 2003. Spontaneous oscillation by hair bundles of the bullfrog's sacculus. *J. Neurosci.* in press.
- Martin, P., and A. J. Hudspeth. 1999. Active hair-bundle movements can amplify a hair cell's response to oscillatory mechanical stimuli. *Proc. Natl. Acad. Sci. USA* 96:14306-14311.
- Martin, P., and A. J. Hudspeth. 2001. Compressive nonlinearity in the hair bundle's active response to mechanical stimulation. *Proc. Natl. Acad. Sci. USA* 98:14386-14391.
- Martin, P., A. J. Hudspeth, and F. Jülicher. 2001. Comparison of a hair bundle's spontaneous oscillations with its response to mechanical stimulation reveals the underlying active process. *Proc. Natl. Acad. Sci. USA* 98:14380-14385.
- Martin, P., A. D. Mehta, and A. J. Hudspeth. 2000. Negative hair-bundle stiffness betrays a mechanism for mechanical amplification by the hair cell. *Proc. Natl. Acad. Sci. USA* 97:12026-12031.
- Narins, P. M., and I. Wagner. 1989. Noise susceptibility and immunity of phase locking in amphibian auditory-nerve fibers. *J. Acoust. Soc. Am.* 85:1255-1265.
- Ospeck, M., V. M. Eguiluz, and M. O. Magnasco. 2001. Evidence of a Hopf bifurcation in frog hair cells. *Biophys. J.* 80:2597-2607.
- Ricci, A. J., and R. Fettiplace. 1997. The effects of calcium buffering and cyclic AMP on mechano-electrical transduction in turtle auditory hair cells. *J. Physiol.* 501:111-124.
- Ricci, A. J., Y. C. Wu, and R. Fettiplace. 1998. The endogenous calcium buffer and the time course of transducer adaptation in auditory hair cells. *J. Neurosci.* 18:8261-8277.
- Strogatz, S. H. 1994. *Nonlinear dynamics and Chaos: with applications to physics, biology, chemistry, and engineering*. Addison-Wesley, Reading, Mass.
- Tilney, L. G., and J. C. Saunders. 1983. Actin filaments, stereocilia, and hair cells of the bird cochlea. I. Length, number, width, and distribution of stereocilia of each hair cell are related to the position of the hair cell on the cochlea. *J. Cell. Biol.* 96:807-821.
- van Netten, S. M., and C. J. Kros. 2000. Gating energies and forces of the mammalian hair cell transducer channel and related hair bundle mechanics. *Proc. R. Soc. Lond. B* 267:1915-1923.
- Wiggins, S. 1990. *Introduction to applied nonlinear dynamical systems and chaos*. Springer-Verlag, New York.
- Wu, Y. C., A. J. Ricci, and R. Fettiplace. 1999. Two components of transducer adaptation in auditory hair cells. *J. Neurophysiol.* 82:2171-2181.